European Journal of Pharmacology 882 (2020) 173255

Contents lists available at ScienceDirect

European Journal of Pharmacology

journal homepage: www.elsevier.com/locate/ejphar

Full length article

Cardioprotection by AN-7, a prodrug of the histone deacetylase inhibitor butyric acid: Selective activity in hypoxic cardiomyocytes and cardiofibroblasts☆

Vadim Nudelman[a,b], Muayad A. Zahalka[a,b], Abraham Nudelman[c], Ada Rephaeli[a,b], Gania Kessler-Icekson[a,b,*]

[a] The Felsenstein Medical Research Center, Rabin Medical Center, Petach-Tikva, Israel
[b] Sackler Faculty of Medicine, Tel-Aviv University, Tel-Aviv, Israel
[c] Department of Chemistry, Bar-Ilan University, Ramat-Gan, Israel

ARTICLE INFO

Keywords:
Histone deacetylase inhibitor
Cardiomyocytes
Cardiofibroblasts
H9c2
Cytoprotection

ABSTRACT

The anticancer prodrug butyroyloxymethyl diethylphosphate (AN-7), upon metabolic hydrolysis, releases the histone deacetylase inhibitor butyric acid and imparts histone hyperacetylation. We have shown previously that AN-7 increases doxorubicin-induced cancer cell death and reduces doxorubicin toxicity and hypoxic damage to the heart and cardiomyocytes. The cardiofibroblasts remain unprotected against both insults. Herein we examined the selective effect of AN-7 on hypoxic cardiomyocytes and cardiofibroblasts and investigated mechanisms underlying the cell specific response. Hypoxic cardiomyocytes and cardiofibroblasts or H_2O_2-treated H9c2 cardiomyoblasts, were treated with AN-7 and cell damage and death were evaluated as well as cell signaling pathways and the expression levels of heme oxygenase-1 (HO-1). AN-7 diminished hypoxia-induced mitochondrial damage and cell death in hypoxic cardiomyocytes and reduced hydrogen peroxide damage in H9c2 cells while increasing cell injury and death in hypoxic cardiofibroblasts. In the cell line, AN-7 induced Akt and ERK survival pathway activation in a kinase-specific manner including phosphorylation of the respective downstream targets, GSK-3β and BAD. Hypoxic cardiomyocytes responded to AN-7 treatment by enhanced phosphorylation of Akt, ERK, GSK-3β and BAD and a significant 6-fold elevation in HO-1 levels. In hypoxic cardiofibroblasts, AN-7 did not activate Akt and ERK beyond the effect of hypoxia alone and induced a limited (~1.5-fold) increase in HO-1. The cell specific differences in kinase activation and in heme oxygenase-1 upregulation may explain, at least in part, the disparate outcome of AN-7 treatment in hypoxic cardiomyocytes and hypoxic cardiofibroblasts.

1. Introduction

Cardiomyocytes are essentially post mitotic and the regenerative capacity of the injured heart remains insignificant. A massive loss of cardiomyocytes is accompanied by increased fibrosis, chamber remodeling and reduced ventricular pumping capability that often deteriorates into heart failure. Heart injury activates cardiofibroblasts to proliferate and secrete extracellular matrix proteins as a reparatory process that maintains the structural integrity of the heart and minimizes myocardial dysfunction and wall rupture. Following the initial wound healing, activated cardiofibroblasts continue to release maladaptive proinflammatory and prohypertrophic signals that result in cardiomyocyte hypertrophy and necrosis and the development of replacement fibrosis (Travers et al., 2016). The critical outcome of cardiomyocyte loss and cardiofibroblast activation emphasizes the need for effective tools that preserve cardiomyocyte viability and restrict cardiofibroblast activation.

Epigenetic mechanisms, including chromatin modifications, represent potential targets for therapeutic intervention. Among which, histone post-translational modifications regulate gene expression and the cell response to environmental stimuli. Histone acetylation status has long been associated with heart pathology underscoring the role of histone deacetylase (HDAC) activity (McKinsey and Olson, 2004; Gallo et al., 2008; Seki et al., 2016; Kang et al., 2015; Renaud et al., 2015).

☆ Performed at the Felsenstein Medical Research Center, Rabin Medical Center, Petach-Tikva, Israel.

* Corresponding author. Felsenstein Medical Research Center, Beilinson Campus, Rabin Medical Center, Petach-Tikva, 49100, Israel.
E-mail addresses: vadimnud@gmail.com (V. Nudelman), zahalka@tauex.tau.ac.il (M.A. Zahalka), abraham.nudelman@biu.ac.il (A. Nudelman), adarephaeli@gmail.com (A. Rephaeli), icekson@tauex.tau.ac.il (G. Kessler-Icekson).

https://doi.org/10.1016/j.ejphar.2020.173255
Received 21 January 2020; Received in revised form 19 May 2020; Accepted 5 June 2020
Available online 15 June 2020

HDAC inhibition may provoke cell death or cell survival, depending on the type of cell and the physiological/pathological condition, as has been shown in cancer cells versus normal cells, in microglia versus neurons, and in cardiomyocytes versus cardiofibroblasts (Tarasenko et al., 2012a, 2012b; Chen et al., 2007; Koko et al., 2017).

AN-7, a prodrug of the HDAC inhibitor butyric acid (BA), is a water-soluble compound that penetrates the cells easily and undergoes metabolic hydrolysis releasing one equivalent of BA. AN-7 is cell selective; it reduces cancer cell viability and augments doxorubicin anti-cancer activity while doing no harm to normal cells and at the same time, protecting cardiomyocytes and the heart against doxorubicin toxicity (Tarasenko et al., 2012a, 2012b, 2017; Rephaeli et al., 2007). Furthermore, AN-7 protected murine hearts against ischemia/reperfusion injury and cardiomyocytes against hypoxia damage that was accompanied by the upregulation of heme oxygenase-1 (HO-1) (Kessler-Icekson et al., 2012). Antifibrotic effects of HDAC inhibition have been reported in various organs including the heart (Renaud et al., 2015; Tarasenko et al., 2017; Hannan et al., 2014; Pang et al., 2009; Park et al., 2014; Sharma et al., 2015; Nural-Guvener et al., 2014). In cardiofibroblasts, AN-7 provoked a damaging effect similar to that observed in cancer cells and in combination with doxorubicin, AN-7 increased ROS production within cardiofibroblasts while diminishing it in similarly treated cardiomyocytes (Tarasenko et al., 2012b).

The selective effect of AN-7 on cardiomyocytes and cardiofibroblasts suggests a bi-faceted role of HDAC inhibition in the heart in case of injury. Herein, we examined differences in the response to AN-7 that confer protection against hypoxia in rat cardiomyocytes while augmenting it in hypoxic co-isolated cardiofibroblasts. The study extends significantly our preliminary observations and provides supportive evidence for disparate impact of AN-7 on signaling pathways and HO-1 expression in the two cell types.

2. Materials and methods

2.1. Cell cultures

The study was approved by the Institutional Committee on the Ethics of Animal Care and Use at Tel-Aviv University (Permits M-08-062 and M-08-037) and conforms to the Consensus Author Guidelines on Animal Ethics and Welfare for Veterinary Journals. Culture media and supplements were from Biological Industries, Beit-Haemek, Israel. Cells were dissociated from ventricles of neonatal Wistar rat hearts (Harlan Laboratories, Jerusalem, Israel) using RDB® as the dissociating enzyme (Israel Institute of Biological Sciences, Ness-Ziona, Israel) (Shalitin et al., 2003; Rephaeli et al., 2007). The isolated cells were suspended in growth medium (DMEM:Ham's F12, 1:1, 5% fetal calf serum (FCS), 5% horse serum (HS), antibiotics) and subjected to differential pre-plating (50 min). Unsettled cells, mostly cardiomyocytes, were collected and seeded (200,000 cells/cm^2) on collagen coated culture dishes (35 mm) or plates (24-well, 96-well) and maintained in a humidified incubator at 37 °C and 95% air/5% CO_2 atmosphere. Spontaneously beating cultures (4–7 days old) were taken for the experiments. The attached cells, mainly cardiofibroblasts (Shalitin et al., 2003), were grown in DMEM, 5% FCS, 5% HS, 2 mM L-glutamine and antibiotics. Confluent cultures were split 1:3 for further cell proliferation and when confluent, cells were transferred to 35 mm dishes (1×10^6 cells/dish), 24-well plates (0.9-1x10^5 cells/well) or 96-well plates (0.1-0.2 $\times$ 10^5 cells/well) and the experiments were performed 24–48 h later at subconfluency. The separation of cardiomyocytes by non-myocyte pre-plating and the enrichment of cardiofibroblasts by two rounds of cell transfer yielded cultures of high cell type homogeneity (Shalitin et al., 2003; Kessler-Icekson et al., 1984). The plating density of each cell type was chosen to maintain best cell viability (the untreated cells) throughout the experiments as well as rhythmic contraction in cardiomyocytes and cell replication in cardiofibroblasts.

To induce hypoxia, cultures were kept in a humidified airtight chamber (Billups-Rothenberg Inc. USA) containing a gas mixture of 1% O_2/5% CO_2/94% N_2, at 37 °C. Oxygen concentration was monitored continuously by a gas detector (BW Technologies, Honeywell, USA). H9c2 embryonic rat cardiomyoblasts were grown to confluency in 100 mm dishes using high glucose DMEM, 10% FCS, 1% L-glutamine and antibiotics as the growth medium. Experiments were conducted on 48 h old cultures in either 35 mm dishes (2.5×10^5/dish) or 24-well plates (0.5×10^5/well). In all the experiments, using the three cell types, AN-7 was added 60 min prior to the induction of hypoxia or the addition of H_2O_2.

2.2. Cell injury and viability

(1) Cell viability: cultures were co-loaded with Hoechst 33342 (H) at 20 μg/ml, and propidium-iodide (PI) at 10 μg/ml; the proportion of PI-labeled (dead), out of H-labeled (total) nuclei was calculated (Kessler-Icekson et al., 2012). (2) Permeability of the mitochondrial permeability transition pores (mPTP): Increased mPTP permeability impairs mitochondrial membrane potential (ΔΨm) and initiates mitochondria-dependent cell death (Hausenloy et al., 2010). To measure mPTP opening, cells (96-well plates) were washed with 40 mM Hepes (pH 7.5) containing 0.65% NaCl and 4.5 g/L glucose, and loaded with calcein-AM (1 μM) (Invitrogen, USA) and $CoCl_2$ (1 mM) in the same buffer. Following 30 min incubation at 37 °C, the cells were washed and the fluorescence of calcein-AM was monitored using excitation/emission filters of 480/528 nm (the Synergy-HT reader, BioTek Industries, USA). (3) Dissipation of ΔΨm (Kessler-Icekson et al., 2012): JC-1 (5,5′,6,6′-tetrachloro-1,1′,3,3′-tetraethylbenzimidazolylcarbo-cyanine iodide) concentrates in energized mitochondria (high membrane potential) and forms red fluorescent aggregates. At low concentrations, in de-energized mitochondria (injured cells), JC-1 monomers emit at the green spectral range. Cells were incubated (30 min, 37 °C) with JC-1 (10 μM) prepared in the same buffer as above, and assessed by (a) fluorescence microscopy employing excitation/emission filters of 460–490/515 nm (green) and 460–490/580 nm (red). Images of 4–5 microscopic fields were analyzed (ImageJ software, NIH, Bethesda, USA) and the proportions of red/green pixels were calculated (R/G); (b) microplate reader (Synergy-HT, BioTek, USA) using excitation/emission filters of 485/528 nm (green) and 545/590 nm (red). The two monitoring methods yielded identical results in calibration experiments.

2.3. Protein and RNA

For Western immunoblotting (WB), cells were harvested in lysis buffer (120 mM Tris-HCl, pH 6.8, 20% glycerol, 10% SDS), boiled (15 min) and sampled for protein quantification (DC protein assay kit, Bio-Rad, USA). DL-Dithiothreitol (10%) and bromophenol blue were added and 30–40 μg protein samples were resolved in 12% or 15% polyacrylamide-SDS gels, electroblotted to Hybond-C Extra membranes (Amersham, UK) and immunolabeled. The primary antibodies were rabbit anti-phospho-Akt, rabbit anti-phospho-GSK-3β, rabbit anti-phospho-BAD (Cell Signaling Technology, USA), mouse anti-phospho-ERK1/2 (Sigma, USA), rabbit anti–HO–1 (Abcam, UK) and mouse anti-β-actin (Santa Cruz Biotechnology, USA). The secondary antibodies, Dylight™800 Goat anti-mouse IgG and Dylight™680 Goat anti-rabbit IgG (Thermo Scientific, USA), were applied as appropriate. Reactive bands were quantified (Odyssey® Infrared Imaging System, Li-Cor Biotechnology, USA) and normalized to the corresponding β-actin band in the same gel-blot.

Extraction of total RNA and preparation of cDNA were as described (Shalitin et al., 2003; Alcalay et al., 2013). Quantitative polymerase chain reaction (qPCR) was performed in 10 μl reactions using the Fast SYBR Green Master Mix and the StepOnePlus Cycler with the StepOnePlus V2.1 software (Applied Biosystems, Invitrogen, USA). In each sample, mRNA levels were obtained from Ct (Cycle threshold) values

and expressed as target gene N-fold difference (ΔCt) from the reference gene *RpS3* (ribosomal protein S3). Differences in mRNA amounts within an experiment were calculated relative to a randomly selected sample of the experiment control group (calculated as $2^{-\Delta\Delta Ct}$) and expressed in Relative Quantity (RQ) values (Alcalay et al., 2013; Kliminski et al., 2017). The primers used were (5′-3′), TGCTCGCATGAACACTCT and TCCTCTTGTCAGCAGTGCC for HO-1, and AAGATGGCCCTGCAGAT TTC and AGCCAGCTCCCGAGTGAGA for *Rps3*.

Protein and mRNA levels are presented as relative values using numerical arbitrary units (AU).

2.4. Statistics

Results are presented as Mean ± SEM. Differences between experimental groups were calculated by one-way analysis of variance (ANOVA) followed by Bonferroni's post-hoc analysis for multiple group comparison. *P* value of < 0.05 was considered statistically significant.

3. Results

3.1. Cell injury and viability

In cardiomyocytes, AN-7 abolished the hypoxia-induced dissipation of ΔΨm maintaining it comparable to that of normoxic cardiomyocytes and even improving ΔΨm status in normoxic cells. However, in cardiofibroblasts, AN-7 increased the hypoxia-induced dissipation of ΔΨm and damaged also normoxic cells (Fig. 1A and B). H9c2 cells were resistant to the experimental hypoxia employed by us, therefore we induced in them oxidative stress using H_2O_2 and found that AN-7 prevented the damage caused by H_2O_2 (Fig. 1A,C).

Complementary tests demonstrated the prevention by AN-7 of mPTP opening and the reduction of cell death in hypoxic cardiomyocytes and their augmentation in hypoxic cardiofibroblasts (Fig. 1D and E), thus substantiating the notion of AN-7 opposing effects in the two cell types.

3.2. Cell signaling

In hypoxic cardiomyocytes, AN-7 enhanced Akt and ERK phosphorylation above the levels induced by hypoxia alone, and the activated state sustained for 8 and 24 h (Fig. 2). GSK-3β and BAD, the respective downstream targets of Akt and ERK, displayed extra-phosphorylation in AN-7-treated hypoxic cardiomyocytes, a modification prevented by the inhibition Akt and ERK activation (Fig. 3). In hypoxic cardiofibroblasts, AN-7 had no significant enhancing effect on Akt or ERK phosphorylation above that induced by hypoxia alone (Fig. 2). Accordingly, no extra-phosphorylation of GSK-3β and BAD was induced by AN-7 (Fig. 3) and Akt and ERK inhibition blocked the hypoxia-induced phosphorylation of GSK-3β and BAD (Fig. 3).

In H9c2 cardiomyoblasts, AN-7 increased further the H_2O_2-induced Akt phosphorylation at 30 min of H_2O_2 treatment, and the phosphorylation of ERK from 15 to 60 min of exposure to H_2O_2 (Fig. 4A–C). Increased GSK-3β and BAD phosphorylation coincided with the related Akt and ERK activation (Fig. 4D and E).

To examine the relevance of Akt and ERK activation for the AN-7-induced cytoprotection, we assessed cell injury while inhibiting Akt and ERK activation. As a result, the AN-7-induced protection of hypoxic cardiomyocytes and H_2O_2-treated cardiomyoblasts was abolished while the injury of hypoxic AN-7-treated cardiofibroblasts was exacerbated (Fig. 5). Namely, Akt and ERK protection pathways are active in the three cell types.

In supplementary experiments, we tested whether the activated Akt affected ERK phosphorylation and vice versa, in the hypoxic AN-7–treated cells. We assessed Akt phosphorylation under the inhibition of ERK activation and ERK phosphorylation under Akt inhibition. As shown in Supplementary Fig. S1, in cardiomyocytes, AN-7-induced Akt

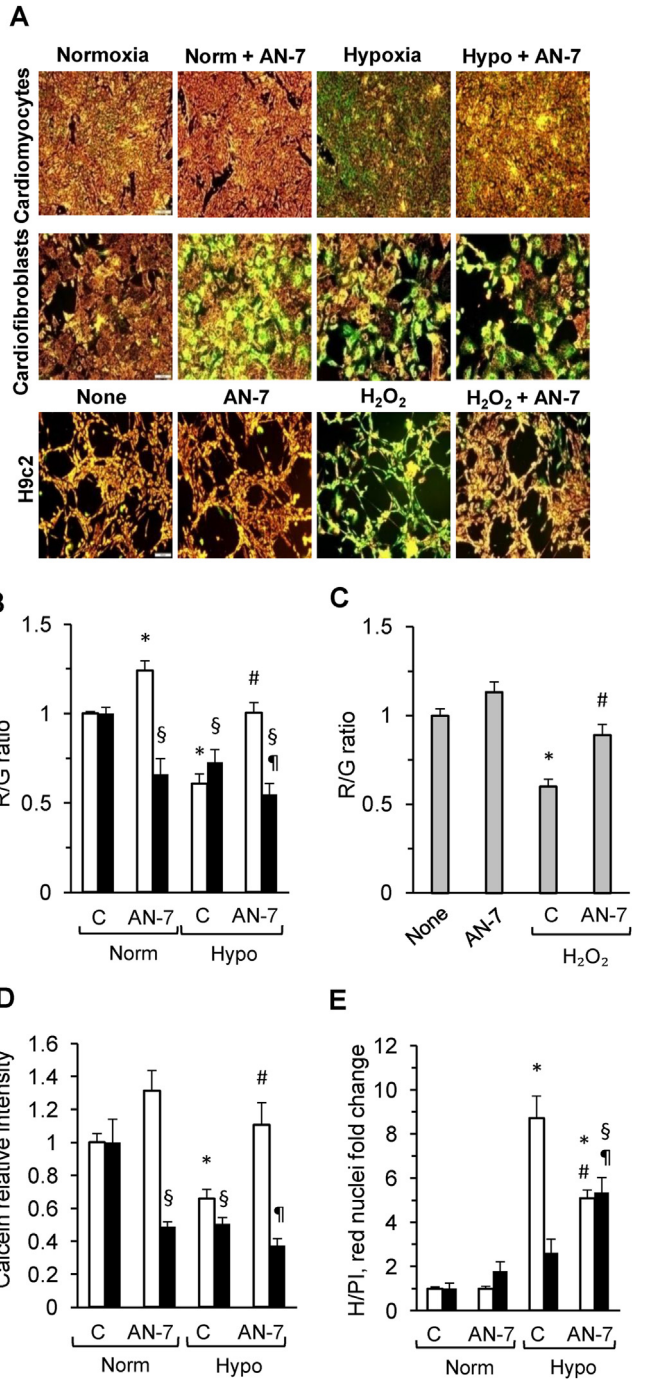

Fig. 1. AN-7 protection, assessment of cell damage and death.
Cardiomyocytes and cardiofibroblasts were subjected to hypoxia and AN-7 (100–150 μM) for 24 h and 48 h, respectively. H9c2 cultures were incubated with H_2O_2 (100 μM, 2 h) and AN-7 (300 μM). **(A-C)** Assessment of ΔΨm by JC-1. **(A)** Representative microscopic images, red, intact cells, green, injured cells. Calibration bar = 100 μm. **(B–C)** The calculated ratio (R/G) of intact (red) to injured (green) cells. **(B)** Cardiomyocytes: $^{*}P < 0.004$ vs. Norm-C; $^{\#}P < 0.0001$ vs. Hypo-C. Cardiofibroblasts: $^{\S}P < 0.02$ vs. Norm-C; $^{\P}P < 0.002$ vs. Hypo-C. **(C)** H9c2 cardiomyoblasts: $^{*}P < 0.0001$ vs. None (untreated control); $^{\#}P < 0.0006$ vs. H_2O_2–C. **(D)** The mPTP status measured as mitochondrial calcein-AM fluorescence intensity, expressed relative to the normoxic control group. Cardiomyocytes, $^{*}P < 0.05$ vs. Norm-C; $^{\#}P < 0.007$ vs. Hypo-C; Cardiofibroblasts, $^{\S}P < 0.002$ vs. Norm-C; $^{\P}P < 0.05$ vs. Hypo-C. **(E)** Cell viability (H-PI labeling) expressed as the ratio of red colored nuclei (dead cells) over total nuclei. Cardiomyocytes, $^{*}P < 0.0001$ vs. Norm-C; $^{\#}P < 0.0001$ vs. Hypo-C; Cardiofibroblasts, $^{\S}P < 0.0001$ vs. Norm-C; $^{\P}P < 0.003$ vs. Hypo-C. Open bars, cardiomyocytes; closed bars, cardiofibroblasts; grey bars, H9c2 cells. Norm, normoxia; Hypo, hypoxia; C, no AN-7;

N = 5–12 cultures/group; Mean ± SEM.

phosphorylation was enhanced by ERK inhibition, suggesting that the activated ERK restricts Akt activation in hypoxic AN-7–treated cardiomyocytes. By contrast, ERK phosphorylation was reduced in response to Akt inhibition, suggesting that the activated Akt regulates positively the parallel activation of ERK. No such relationships were found in hypoxic AN-7-treated cardiofibroblasts.

We conclude that activation of Akt and ERK signaling pathways mediate the AN-7-induced cytoprotection in hypoxic cardiomyocytes and in H_2O_2-injured H9c2 cardiomyoblasts. In cardiofibroblasts, the two kinases sustain a basal level of protection that is not sufficient to prevent hypoxia damage alone and in combination with AN-7.

3.3. HO-1 function and expression

Our preliminary findings that HO-1 is upregulated in AN-7-protected cardiomyocytes called for the examination of HO-1 function in AN-7 protection (Kessler-Icekson et al., 2012). Zinc protoporphyrin-IX (ZnPP) is a synthetic heme derivative that acts as a competitive HO-1 inhibitor (Ryter et al., 2006). Inhibition of HO-1 activity by ZnPP abolished the protection imparted by AN-7 to hypoxia-treated cardiomyocytes and H_2O_2-treated H9c2 cardiomyoblasts, while exacerbating further the damage caused to hypoxia-treated cardiofibroblasts (Fig. 6A and B). It is suggested that AN-7 protection is mediated by HO-1 in both, hypoxic cardiomyocytes and H_2O_2-injured cardiomyoblasts. In cardiofibroblasts where AN-7 does not impart protection, a detectable ZnPP-enhanced cell death indicates an existing HO-1 protection that

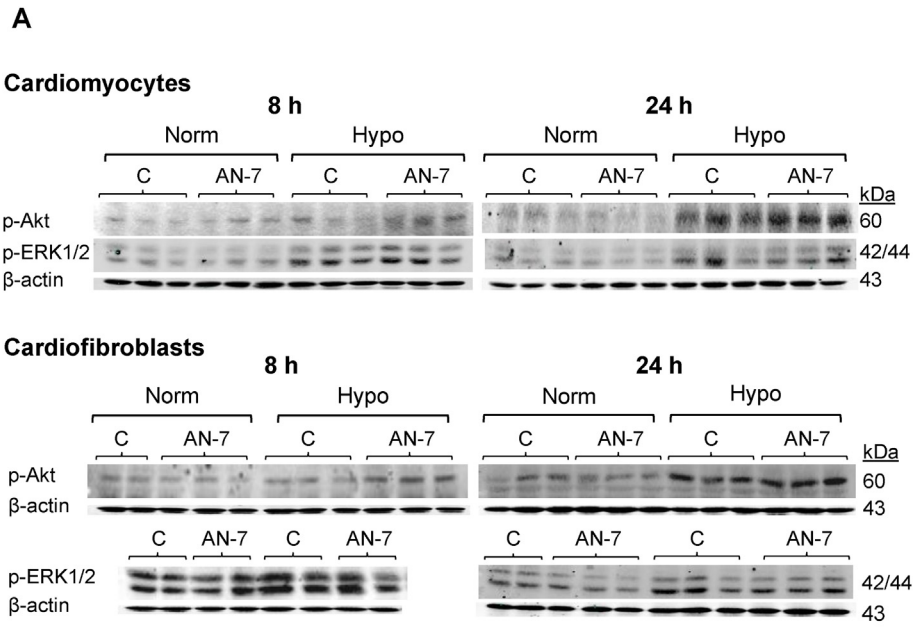

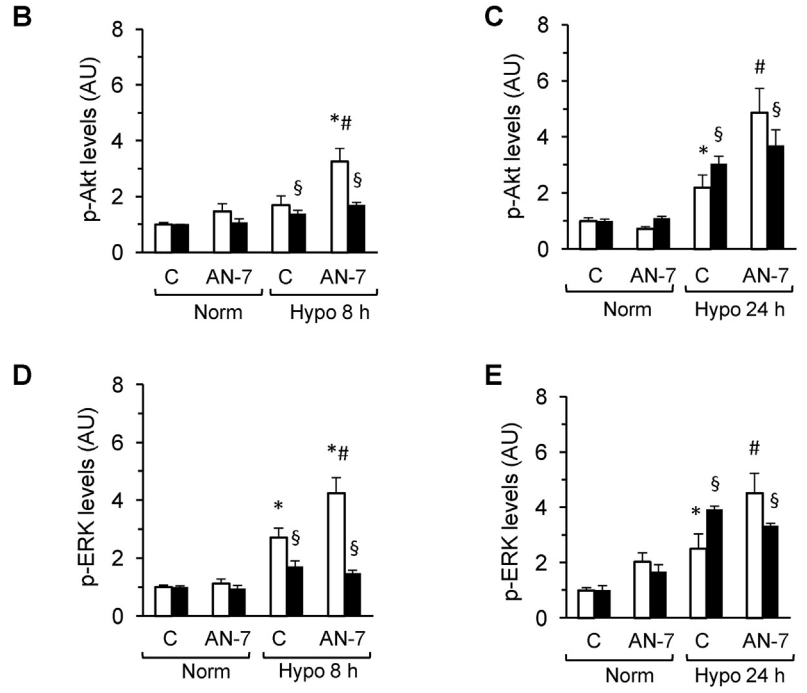

Fig. 2. Akt and ERK phosphorylation. Cells were subjected to 8 or 24 h of hypoxia and AN-7 (150 μM). Phosphorylated kinases were assessed by WB. **(A)** Representative immunoblots. **(B)** Phospho-Akt, 8 h. Cardiomyocytes, *P < 0.001 vs. Norm-C; #P < 0.05 vs. Hypo-C. Cardiofibroblasts, §P < 0.05 vs. Norm-C. **(C)** Phospho-Akt, 24 h. Cardiomyocytes, *P < 0.003 vs. Norm-C; #P < 0.002 vs. Hypo-C; Cardiofibroblasts, §P < 0.0008 vs. Norm-C; **(D)** Phospho-ERK1/2, 8 h. Cardiomyocytes, *P < 0.05 vs. Norm-C; #P < 0.05 vs. Hypo-C. Cardiofibroblasts, §P < 0.001 vs. Norm-C. **(E)** Phospho-ERK1/2, 24 h. Cardiomyocytes, *P < 0.02 vs. Norm-C; #P < 0.05 vs. Hypo-C. Cardiofibroblasts, §P < 0.008 vs. Norm-C; Open bars, cardiomyocytes; closed bars, cardiofibroblasts. Norm, normoxia; Hypo, hypoxia; C, no AN-7. N = 3–11 cultures/group. Mean ± SEM. AU, arbitrary units.

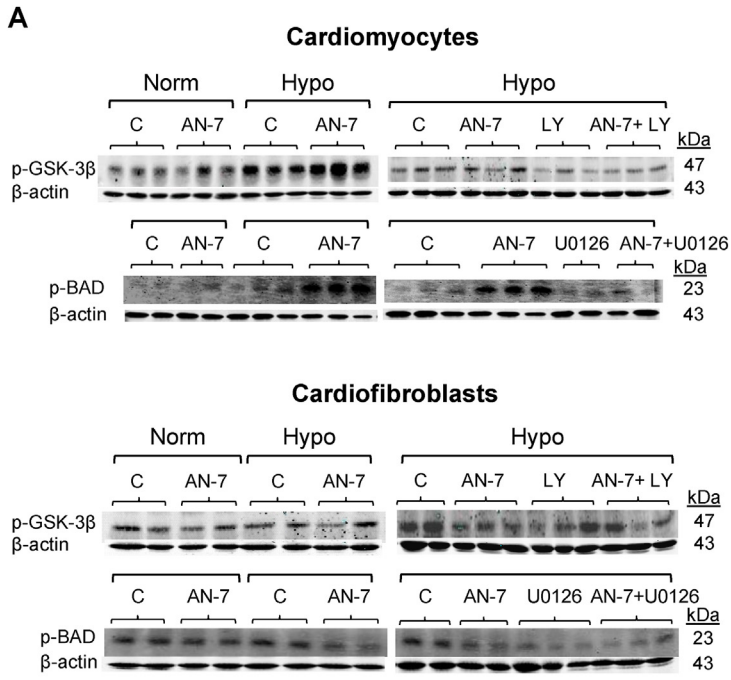

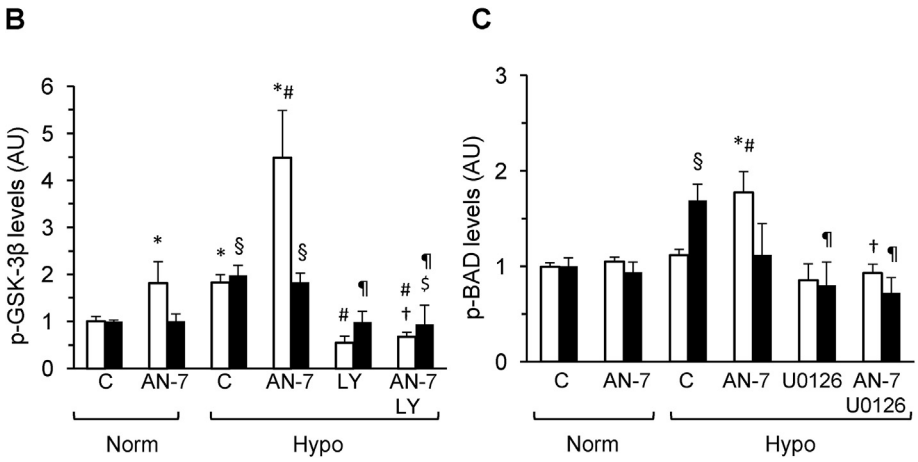

Fig. 3. GSK-3β and BAD phosphorylation. The cells underwent combined hypoxia and AN-7 (150 μM) treatment for 8 h in the presence of Akt inhibitor (LY-294002, 20 μM) or ERK inhibitor (U0126, 10 μM). Phosphorylated GSK-3β and BAD were assessed by WB. **(A)** Representative immunoblots. **(B)** Phospho-GSK-3β. Cardiomyocytes, *P < 0.006 vs. Norm; #P < 0.05 vs. Hypo-C; †P < 0.0006 vs. Hypo + AN-7. Cardiofibroblasts, §P < 0.05 vs. Norm, ¶P < 0.05 vs. Hypo-C; $P < 0.0005 vs. Hypo + AN-7. **(C)** Phospho-BAD. Cardiomyocytes, *P < 0.05 vs. Norm; #P < 0.05 vs. Hypo-C; †P < 0.01 vs. Hypo + AN-7. Cardiofibroblasts. §P < 0.001 vs. Norm; ¶P < 0.05 vs. Hypo-C. Open bars, cardiomyocytes; closed bars, cardiofibroblasts. Norm, normoxia, Hypo, hypoxia; C, no AN-7. N = 5–11 cultures/group. Mean ± SEM. AU, arbitrary units.

cannot rescue the cells from hypoxia or hypoxia plus AN-7 injury (Fig. 6A).

Hypoxia upregulated the levels of HO-1 mRNA and protein in both, cardiomyocytes and cardiofibroblasts that increased further when AN-7 was added (Fig. 6C–E). The AN-7 effect on HO-1 mRNA was abolished by the inhibition of AKT and not of ERK activation (Fig. 6D). However, the increase in the protein was susceptible to inhibition of either AKT or ERK activation in the two cell types (Fig. 6E). Namely, in the AN-7 treated cells, the ERK pathway regulates the amount of HO-1 protein rather than the mRNA.

The changes in HO-1 protein over time did not fully overlap those in the mRNA and the extent of increase was greater in cardiomyocytes compared with cardiofibroblasts (Fig. 7). Increased mRNA levels were detectable already at 4 h, and at 8 h, the presence of AN-7 in hypoxic cells nearly doubled the mRNA levels induced by hypoxia alone. At 8 h, the cardiomyocytes manifested ~10-fold and ~20-fold increase in HO-1 mRNA in hypoxia and hypoxia + AN-7-treated cells, respectively, whereas similarly treated cardiofibroblasts manifested only ~3-fold and ~8-fold increase, respectively (Fig. 7A). At 24 h, the AN-7 enhancing effect over hypoxia alone disappeared (Fig. 7A). As for the protein, in hypoxia and hypoxia plus AN-7-treated cardiomyocytes, the relative increase over normoxia was ~5-fold and ~10-fold at 8 h, and ~3-fold and ~17-fold at 24 h, respectively. In hypoxia and hypoxia plus AN-7-treated cardiofibroblasts, the relative increase in HO-1 was ~2-fold and ~2-fold at 8 h, and ~5-fold and ~7-fold at 24 h, respectively (Fig. 7B). In all, the regulation of HO-1 expression in hypoxic AN-7-treated cardiomyocytes and cardiofibroblasts follows a similar pattern with apparent quantitative differences that point to superior HO-1 protection in cardiomyocytes. Despite the evidence of a protective effect of HO-1 in H_2O_2 - and AN-7 -treated H9c2 cells, assessment of HO-1 mRNA or protein did not reveal any significant changes over 2 h of the experiments (not shown). Whether AN-7 affected HO-1 activity rather than stability or synthesis awaits further investigation.

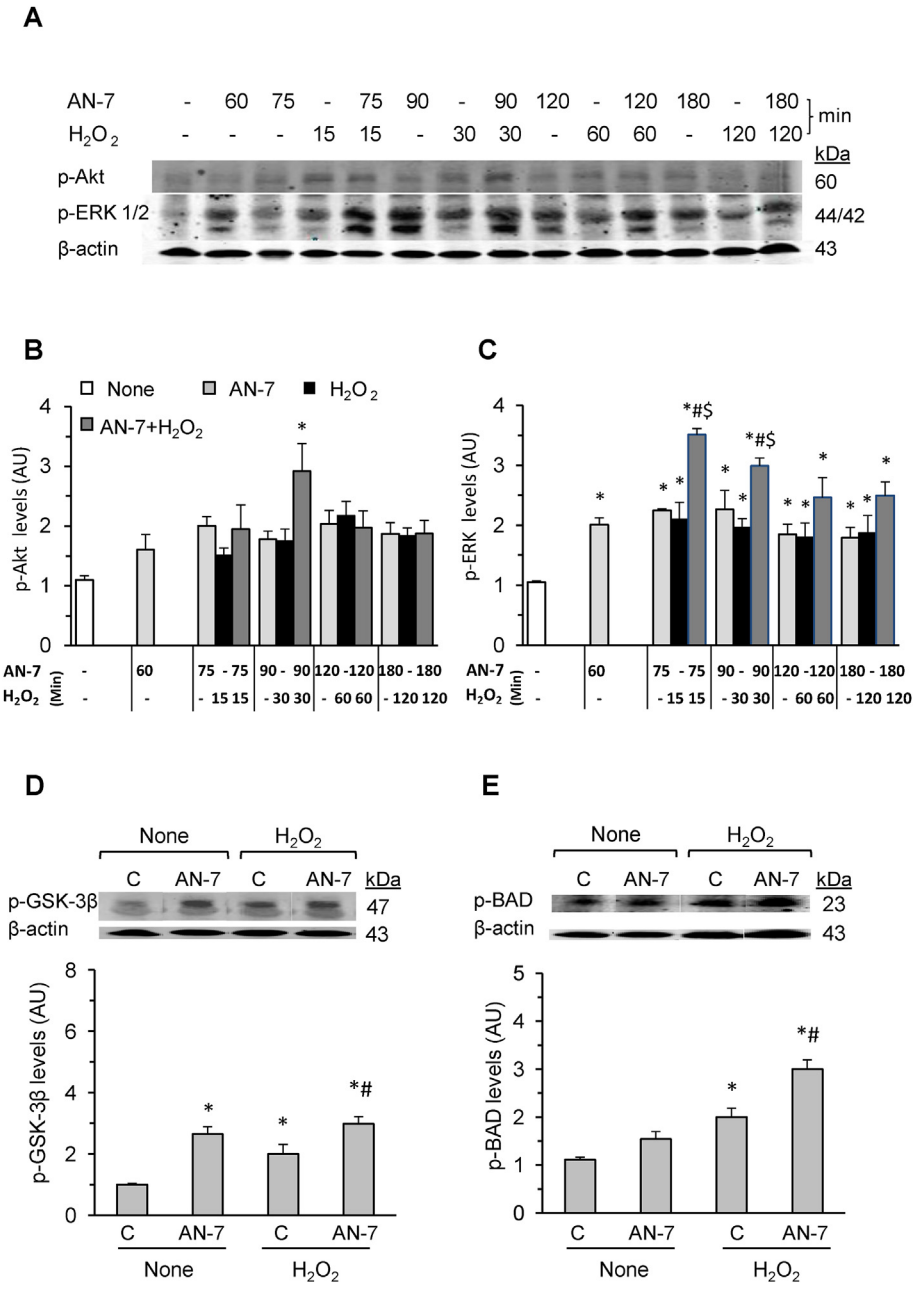

Fig. 4. AN-7-induced kinase phosphorylation in H9c2 cardiomyoblasts. Cells were incubated with AN-7 (300 μM) for 60 min then H_2O_2 (100 μM) was added for increasing durations. Phosphorylated kinases were assessed by WB. **(A)** Representative immunoblots. **(B)** Phospho-Akt, *P < 0.002 vs. None (untreated control). **(C)** Phospho-ERK, *P < 0.02 vs. None; #P < 0.002, vs. the corresponding H_2O_2; $P < 0.04 vs. the corresponding AN-7. **(D)** Phospho-GSK-3β in cultures treated with AN-7 for 90 min, of which the last 30 min were in combination with H_2O_2. *P < 0.008 vs. None-C; #P < 0.02 vs. H_2O_2–C. **(E)** Phospho-BAD in cultures treated with AN-7 for 75 min, of which the last 15 min in combination with H_2O_2. *P < 0.006 vs. None-C; #P < 0.002 vs. H_2O_2–C. In **D**, and **E**, the bands presented were cut and rearranged from an individual gel blot of a distinct experiment, including the corresponding actin bands; None, no H_2O_2; C, no AN-7. N = 3–14 cultures/group. Mean ± SEM. AU, arbitrary units.

4. Discussion

4.1. Cell selective action of AN-7

In this study, we have demonstrated that AN-7 elicits opposite effects in cardiomyocytes and cardiofibroblasts exposed to the stress of oxygen deprivation. In hypoxic cardiomyocytes, AN-7 preserved the mitochondrial status, preventing opening of the mPTP and ΔΨm dissipation, and reduced cell death. Although AN-7 maintained the mitochondrial status at normoxia levels, cell viability was not fully restored (~50%) possibly due to activity of mitochondria-independent death pathways (Sinha et al., 2013). AN-7 improved mitochondria status also in normoxic cells, reducing apparently unfavorable effects of culture conditions as such. In the cardiofibroblasts, AN-7 increased hypoxia damage to the mitochondria, aggravated cell death and reduced viability of normoxic cells. The AN-7 protection of cardiomyocytes and its toxicity to cardiofibroblasts corroborate previous findings in doxorubicin-treated cells (Rephaeli et al., 2007).

The H9c2 cell line of an embryonic rat heart origin is widely used as a model for studies on heart cell injury and viability (Lenčo et al., 2015). AN-7 protected H9c2 cells against H_2O_2 injury, similar to AN-7 protection against doxorubicin toxicity (Tarasenko et al., 2012b).

4.2. Akt and ERK activation

Published observations indicate that HDAC inhibition may involve activation and/or deactivation of signaling pathways (Rahmani et al., 2005; Yao et al., 2012; Correa et al., 2011; Zhu et al., 2011). In hypoxic cardiomyocytes, AN-7 induced phosphorylation of Akt and ERK to much above their phosphorylation in normoxic or hypoxic cells, during at least 24 h, including a parallel phosphorylation of GSK-3β and BAD. The AN-7-induced kinase phosphorylation and cell protection depended on Akt and ERK activation and were blocked by Akt and ERK phosphorylation-inhibitors. In hypoxic cardiofibroblasts, treatment with AN-7 did not enhance Akt and ERK or GSK-3β and BAD phosphorylation beyond the effect of hypoxia alone. Nonetheless, the inhibition

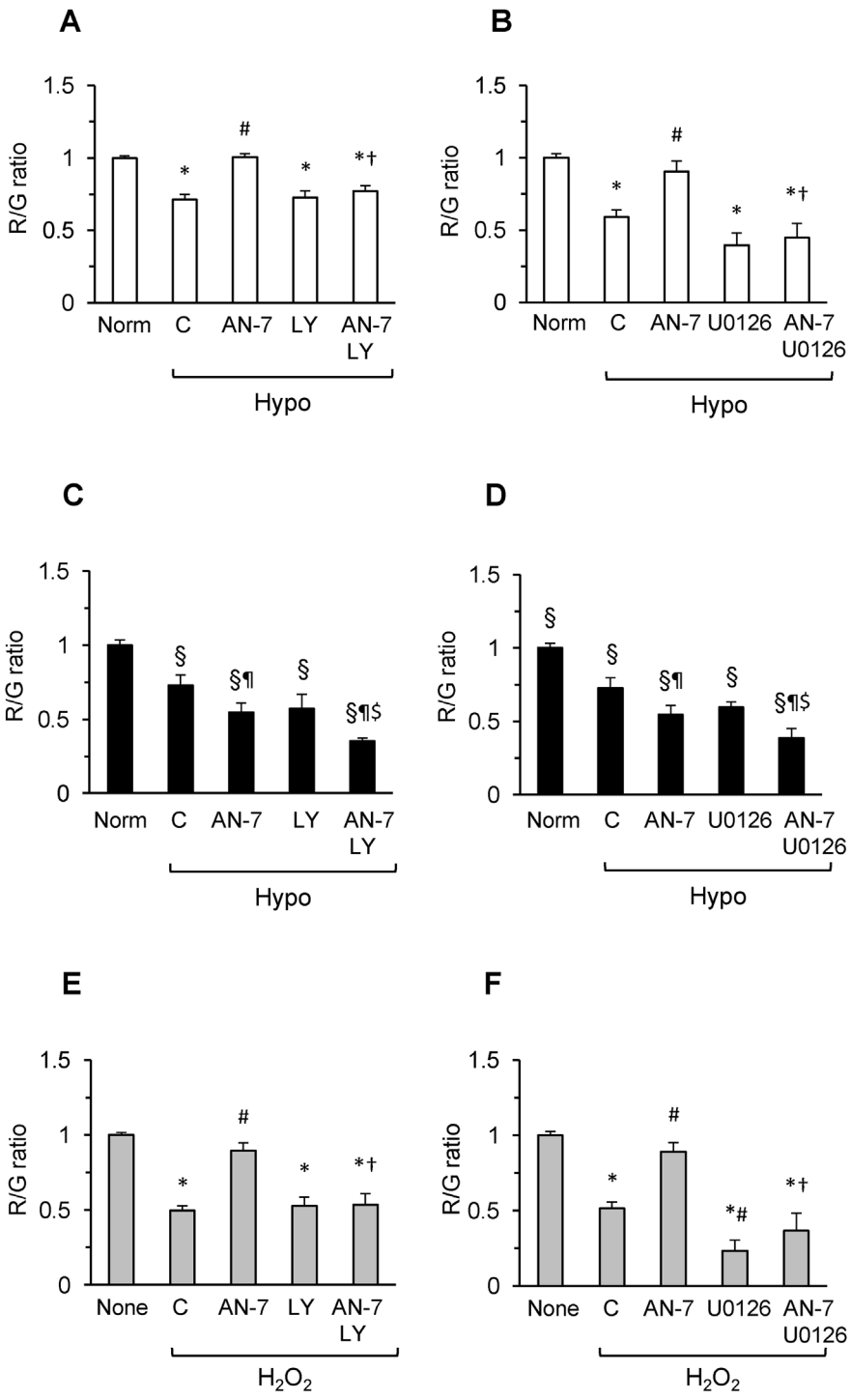

Fig. 5. Akt and ERK inhibition abolishes AN-7 effects. Cardiomyocytes and cardiofibroblasts were subjected to hypoxia and AN-7 (150 μM) for 24 h and 48 h, respectively, in the presence of LY-294002 (20 μM) or U0126 (10 μM). Cell survival was measured using JC-1, calculating the ratio of red (intact) over green (injured) cells (R/G). **(A)** Akt, and **(B)** ERK, inhibition in cardiomyocytes. *P < 0.0001 vs. Norm; #P < 0.0002 vs. Hypo-C; †P < 0.0001 vs. Hypo + AN-7. **(C)** Akt, and **(D)**, ERK inhibition in cardiofibroblasts. §P < 0.05 vs. Norm; ¶P < 0.04 vs. Hypo-C; $P < 0.05 vs. Hypo + AN-7. **(E)** Akt, and **(F)** ERK, inhibition in H9c2 cells. Cells were treated with AN-7 (300 μM) for 180 min, of which the last 120 min in combination with H_2O_2 (100 μM), in the presence of LY-294002 or U0126 (20 μM each). *P < 0.0001 vs. None; #P < 0.03 vs. H_2O_2–C; †P < 0.0001 vs. H_2O_2 + AN-7. Open bars, cardiomyocytes; closed bars, cardiofibroblasts; grey bars, H9c2 cells. Norm, normoxia, Hypo, hypoxia; None, no H_2O_2; C, no AN-7. N = 3–18 cultures/group; Mean ± SEM.

experiments indicated that Akt and ERK signaling afforded some protection to hypoxic cardiofibroblasts that was not sufficient to rescue the cells from the damage inflicted by hypoxia and AN-7.

GSK-3β and BAD contribution to cell survival depends on their phosphorylation status. GSK-3β mediates cell protection through the phosphorylation of Ser9 that modulates GSK-3β interaction with mPTP complexes to reduce the probability of mPTP opening and prevent the dissipation of ΔΨm and cell death (Juhaszova et al., 2009). Phosphorylation of BAD provokes Bcl-2 translocation from the cytosol to the mitochondria where it prevents mPTP opening, maintains ΔΨm, and preserves cell viability. Cytosolic phospho-BAD is sequestered further by binding to 14-3-3 proteins that helps prevent apoptosis (Liu et al., 2014).

H_2O_2, a known activator of MAP kinases, induced in H9c2 cells a kinase specific Akt and ERK activation. When combined with AN-7, the kinase response to H_2O_2 was modified mainly by increasing the peak activation and prolonging the duration of the activated state. Parallel phosphorylation of GSK-3β and BAD played, apparently, a protective role in the H_2O_2-challenged-AN-7-treated H9c2 cells. The experiments in H9c2 cells demonstrated rapid kinase phosphorylation in response to AN-7, that may allude to acetylation of kinases, phosphatases or their regulators (Kang et al., 2015; Spange et al., 2009; Zhao et al., 2007; Hsu et al., 2011; Ryter et al., 2002).

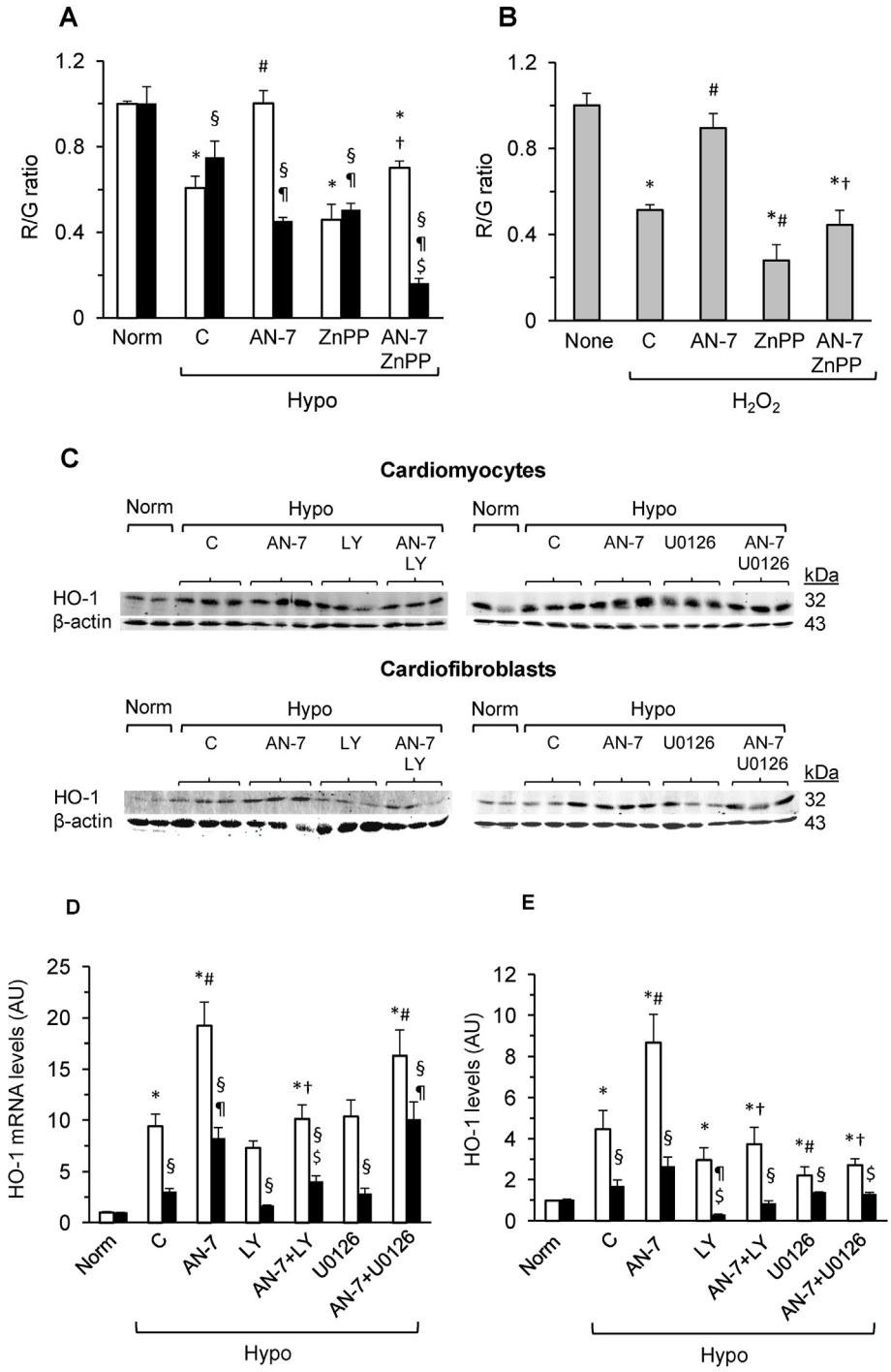

Fig. 6. HO-1 protection and regulation of expression. Cardiomyocytes and cardiofibroblasts were treated with AN-7 (150 μM) and ZnPP (2 μM, and 1 μM, respectively) and exposed to hypoxia for 24 h (cardiomyocytes) and 48 h (cardiofibroblasts). H9c2 cells received AN-7 (300 μM) and ZnPP (1.5 μM) and were exposed to H_2O_2 (100 mM) for 2 h. **(A–B)** Cell viability, JC-1 labeling. R/G, red (intact) over green (injured) cells. **(A)** Cardiomyocytes, *P < 0.001 vs. Norm; #P < 0.001 vs. Hypo-C; †P < 0.001 vs. Hypo + AN-7. Cardiofibroblasts, §P < 0.05, vs. Norm; ¶P < 0.05 vs. Hypo-C; $P < 0.001 vs. Hypo + AN-7. **(B)** H9c2 cells, *P < 0.001 vs. None; #P < 0.05 vs. H_2O_2–C; $P < 0.001 vs. H_2O_2 + AN-7. **(C–E)** HO-1 expression. Cardiomyocytes and cardiofibroblats were exposed to 8 h hypoxia and AN-7 (150 μM) in the presence of LY- 294002 (20 μM) or U0126 (10 μM). HO-1 mRNA and protein were assessed by qPCR and WB, respectively. **(C)** Representative immunoblots. **(D)** HO-1 mRNA. Cardiomyocytes, *P < 0.05 vs. Norm; #P < 0.05 vs. Hypo-C; †P < 0.05 vs. Hypo + AN-7. Cardiofibroblasts, §P < 0.05 vs. Norm; ¶P < 0.05 vs. Hypo-C; $P < 0.05 vs. Hypo + AN-7; **(E)** HO-1 protein. Cardiomyocytes, *P < 0.05 vs. Norm; #P < 0.05 vs. Hypo-C; †P < 0.05 vs. Hypo + AN-7. Cardiofibroblasts, §P < 0.05 Norm; ¶P < 0.05 vs. Hypo-C; $P < 0.05 vs. Hypo + AN-7; Open bars, cardiomyocytes; closed bars, cardiofibroblasts; grey bars, H9c2 cells. Norm, normoxia; Hypo, hypoxia; C, no AN-7. N = 3–11 cultures/group; Mean ± SEM. AU, arbitrary units.

4.3. HO-1 function and regulation

HO-1 provides cytoprotection through production of the anti-oxidants biliverdin/bilirubin and the anti-inflammatory carbon monoxide that also helps iron excretion from the cells (Ryter et al., 2002, 2006). HO-1 expression is relatively low and is upregulated rapidly in response to stress conditions such as hypoxia and inflammation (Ryter et al., 2002; Wang et al., 2010). HO-1 protects the heart against oxidative stress, ischemia/reperfusion injury and heart failure (Wang et al., 2010; Choi and Kim, 2008). Kinase-activated signaling pathways, including Akt and ERK, mediate HO-1 induction by activating diverse transcription factors and response elements, particularly the Nrf2 transcription factor (Choi and Kim, 2008; Wang et al., 2012; Dong et al., 2017). HDAC inhibition has been shown to impart cerebral protection against ischemia and diabetic nephropathy through Nrf2 activation and HO-1 upregulation (Wang et al., 2012; Dong et al., 2017). Besides, Akt activation has been shown to directly modulate HO-1 activity via phosphorylation at Ser188 (Salinas et al., 2004).

Early evidence from our laboratory indicated the upregulation of HO-1 expression in AN-7-treated isolated hearts exposed to ischemia/reperfusion and in cardiomyocytes under hypoxia (Kessler-Icekson et al., 2012). Herein, we extended the preliminary study confirming the importance of HO-1 for cardiomyocyte protection and investigating aspects of the AN-7-regulated HO-1 expression. HO-1 inhibition abrogated AN-7 protection in hypoxic cardiomyocytes and aggravated hypoxia and AN-7 damage to cardiofibroblasts. Namely, HO-1 plays a

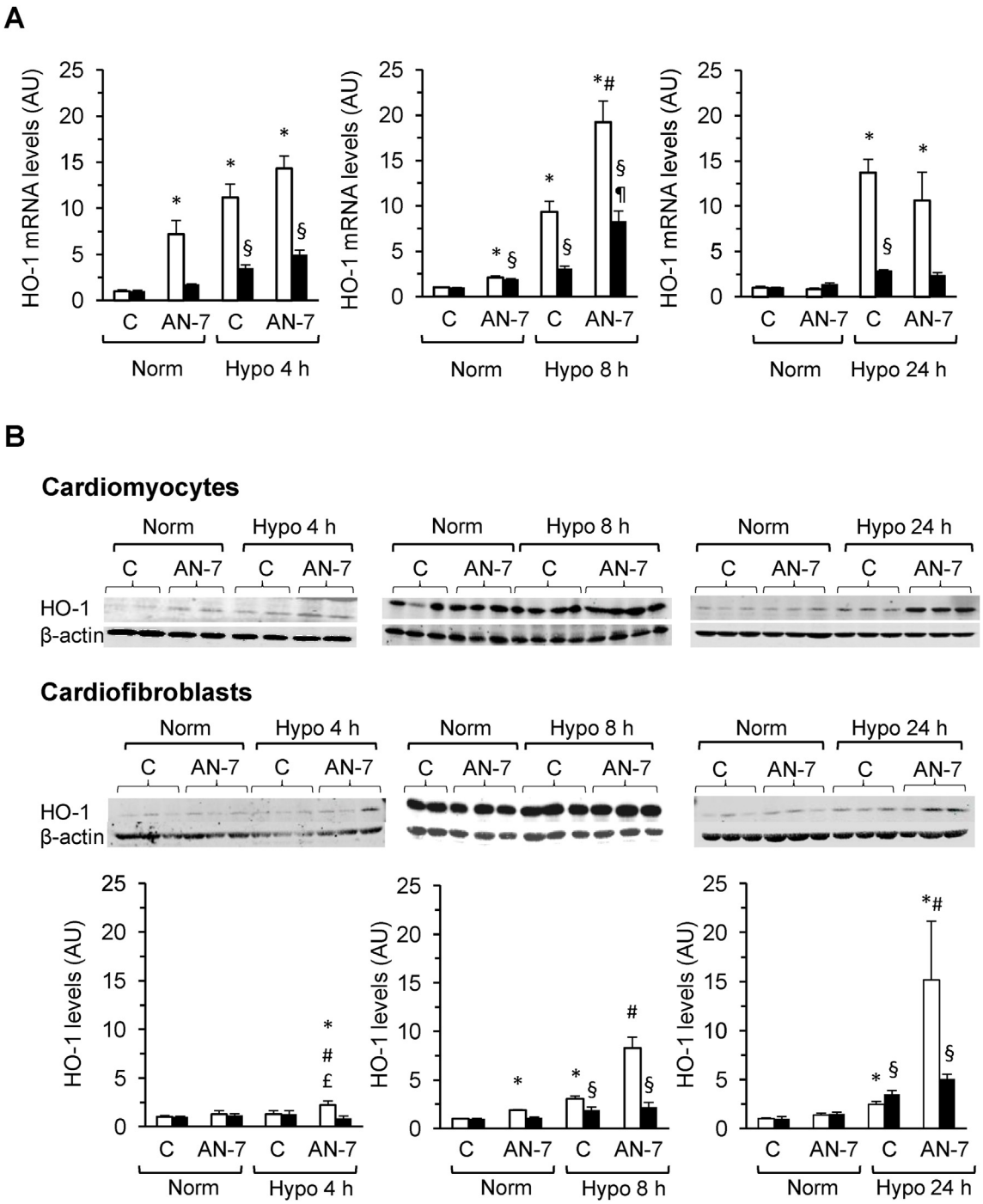

Fig. 7. Changes over time in HO-1 expression. Cardiomyocytes and cardiofibroblasts underwent 4, 8, and 24 h hypoxia with AN-7 (100–150 μM). HO-1 mRNA and protein levels were assessed by RT-qPCR and WB, respectively. (**A**) Relative levels of HO-1 mRNA. Cardiomyocytes, *P < 0.05 vs. Norm-C; #P < 0.005 vs. Hypo-C. Cardiofibroblasts, §P < 0.05 vs. Norm-C; ¶P < 0.005 vs. Hypo-C. **(B)** Relative levels of HO-1 protein. Upper panel, representative immunoblots. Lower panel, summary of band quantification. Cardiomyocytes: At 4 h, *P < 0.05 vs. Norm-C; #P < 0.05 vs. Hypo-C. £P < 0.05 vs. Norm + AN-7. At 8 h, *P < 0.05 vs. Norm-C; #P < 0.005 vs. Hypo-C. At 24 h, *P < 0.05 vs. Norm-C; #P < 0.005 vs. Hypo-C. Cardiofibroblasts: §P < 0.05 vs. Norm-C; Open bars, cardiomyocytes; closed bars, cardiofibroblasts. Norm, normoxia; Hypo, hypoxia; C, no AN-7. N = 5–13 cultures/group. Mean ± SEM. AU, arbitrary units.

protector role in both, hypoxic cardiomyocytes and cardiofibroblasts, yet, in the latter cells, HO-1 activity cannot ameliorate the outcome of hypoxia and AN-7.

Hypoxia upregulated HO-1 mRNA in cardiomyocytes at all the time points tested and the addition of AN-7 elevated it further. At 8 h hypoxia, AN-7 doubled the effect of hypoxia alone. HO-1 protein content was elevated as well during the 24 h follow-up. The hypoxia stress was not mandatory for the AN-7 effect since the prodrug enhanced HO-1 expression also in normoxic cardiomyocytes at 4–8 h of treatment. A temporal and quantitative discrepancy between the changes in the mRNA and the protein suggests higher stability of the protein that may be attributed to a regulatory effect of HDAC inhibition on mechanisms of protein degradation (Tarasenko et al., 2017; Chi et al., 2019). The general pattern of HO-1 elevation was similar in cardiomyocytes and cardiofibroblasts although quantitative differences distinguished the two cell types, the elevation being markedly smaller in the

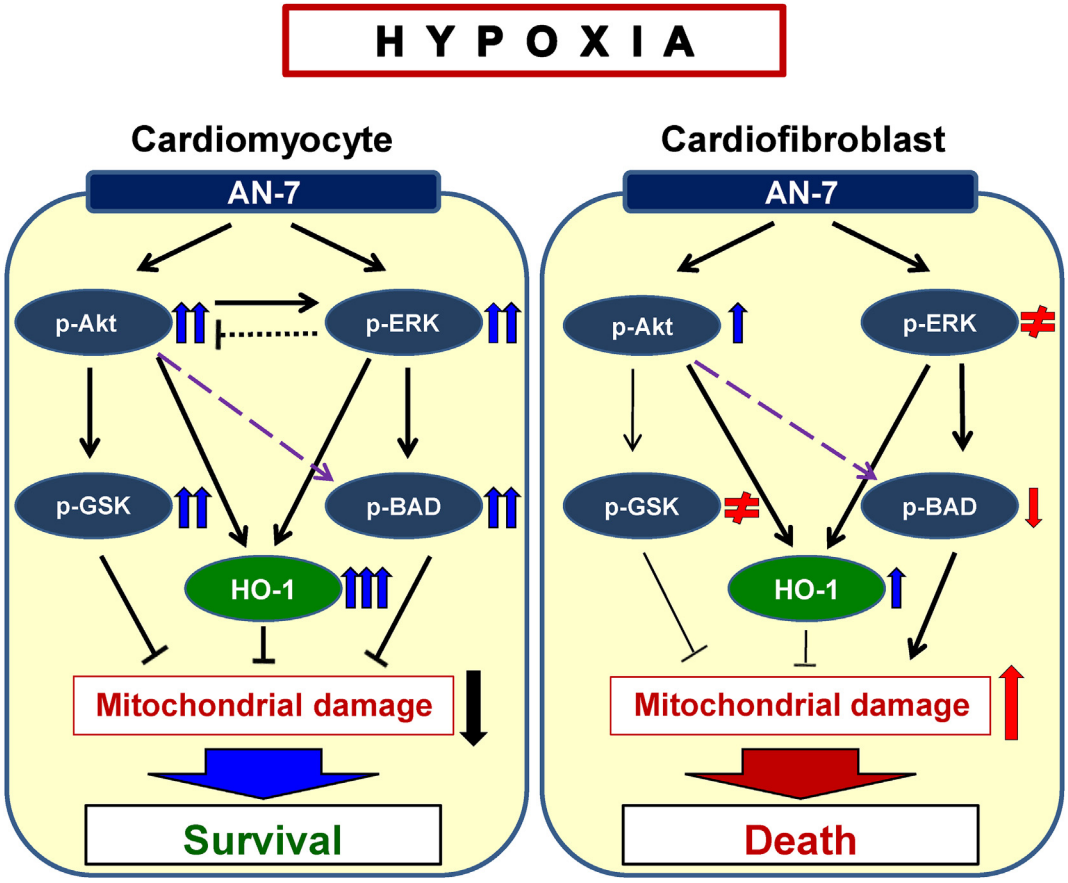

Fig. 8. Schematic representation of AN-7 action in a hypoxic cardiomyocyte and cardiofibroblast. In the cardiomyocyte, AN-7 activates the kinases Akt and ERK that phosphorylate their downstream targets GSK-3β and BAD that help preserve cell viability. Concomitantly, Akt and ERK signal HO-1 upregulation that provides additional protection against hypoxia. Cell viability is preserved.
In the cardiofibroblast, AN-7 has little effect on Akt and ERK activation and no downstream impact on GSK-3β and BAD phosphorylation. HO-1 upregulation is small. No significant protection is achieved.
Standard black arrows indicate pathway direction. Purple arrows refer to published knowledge not tested by us. Bold arrows indicate the type (up/down) and the extent (arrow size and number) of change. ≠, means no change.

cardiofibroblasts compared to cardiomyocytes. A similar discrepancy in HO-1 levels was reported in AN-7 and doxorubicin treated cardiomyocytes and cardiofibroblasts (Tarasenko et al., 2012b). Since the amount of cellular HO-1 and the ability to recruit additional HO-1 upon injury, are vital for cell survival, the low increase in HO-1 may limit the ability of AN-7 to protect cardiofibroblasts against hypoxia.

In hypoxic cardiomyocytes, Akt inhibition interfered with the AN-7-induced production of HO-1 mRNA whereas ERK inhibition did not. Nonetheless, the inhibition of both, Akt and ERK, reduced the amount of HO-1 protein in hypoxic cardiomyocytes and abolished completely the supplementary elevation induced by AN-7. The observation that ERK inhibition allows extra Akt phosphorylation suggests a compensatory increase in Akt activation (and HO-1 upregulation) under ERK inhibition (Fig. S1). Alternatively, the activated ERK might not be essential for the increase in HO-1 mRNA and still control the protein synthesis or stability, as was reported in pulmonary epithelial cells exposed to a lipid peroxidation product (Iles et al., 2005). Likewise, in hypoxic cardiofibroblasts, Akt inhibition affected the regulation of HO-1 mRNA and the protein while ERK inhibition affected the protein only.

4.4. Conclusions

The novelty of our study resides with the elucidation of AN-7 action in hypoxic cardiomyocytes and cardiofibroblasts derived from the same hearts. The activation of Akt and ERK and the consequential, protective, GSK-3β and BAD phosphorylation along with the upregulation of HO-1, afford cardiomyocyte survival. In the cardiofibroblasts, the above listed changes are either absent or of much smaller magnitude. These differences likely account for the disparate effect of AN-7 on cardiomyocyte and cardiofibroblast survival when facing hypoxia (summarized in Fig. 8).

4.5. Study limitations and future perspectives

While the study substantiated the opposite effect of AN-7 on hypoxic cardiomyocytes and cardiofibroblasts, and provided several insights into the processes involved, it has not presented a conclusive explanation as to the mechanisms underlying the selectivity, nor did it clarify why AN-7 enhances damage to cardiofibroblasts. The detailed regulation, by AN-7, of mitochondria-dependent death/survival pathways awaits further investigation as well as the detailed mechanism(s) through which AN-7 controls kinase activation and HO-1 expression in each of the heart-derived cell populations, including the possible role of diverse acetylated proteins.

Author agreement declaration

The Corresponding Author certifies that all authors have seen and approved the final version of this manuscript. The article is the authors' original work, has not been published previously (except in the form of a conference abstract) and is not under consideration for publication elsewhere.

CRediT authorship contribution statement

Vadim Nudelman: Formal analysis, Writing - original draft. **Muayad A. Zahalka:** Formal analysis. **Abraham Nudelman:** Prodrug design and synthesis, Funding acquisition. **Ada Rephaeli:** Conceptualization, Funding acquisition, Editing - original draft. **Gania Kessler-Icekson:** Conceptualization, Funding acquisition, Supervision, Writing - original draft.

Declaration of competing interest

The Authors declare that there is no conflict of interest.

Acknowledgements

The work was performed in partial fulfillment of the requirements for a PhD degree of Vadim Nudelman at The Sackler Faculty of Medicine, Tel-Aviv University, Israel. The authors thank Mrs. Hadassa Schlesinger for assistance in part of the experiments. Financial support: The Israeli Ministry of Sciences and Arts (Grant No. 01-01-01449, to G.K–I., A.N. and A.R.); The Chief Scientist Office in the Israeli Ministry of Health (Grant No. 3780, to G.K–I.); The Sackler Faculty of Medicine, Tel-Aviv University (to G.K–I.).

Appendix A. Supplementary data

Supplementary data to this article can be found online at https://doi.org/10.1016/j.ejphar.2020.173255.

References

Alcalay, Y., Hochhauser, E., Kliminski, V., Dick, J., Zahalka, M.M., Parnes, D., Schlesinger, H., Abassi, Z., Shainberg, A., Schindler, R.F., Brand, T., Kessler-Icekson, G., 2013. Popeye Domain Containing 1 (Popdc1/Bves) is a caveolae-associated protein involved in ischemia tolerance. PloS One 8, e71100.

Chen, P.S., Wang, C.C., Bortner, C.D., Peng, G.S., Wu, X., Pang, H., Lu, R.B.P., Gean, W., Chuang, D.M., Hong, J.S., 2007. Valproic acid and other histone deacetylase inhibitors induce microglial apoptosis and attenuate lipopolysaccharide-induced dopaminergic neurotoxicity. Neuroscience 149, 203–212.

Chi C., Z., Byeon, H.-E., Seo, E., Nguyen, Q.-A.T., Lee, W., Jeong, Y., Choi, J., Pandey, D., Berkowitz, D.E., Kim, J.H., Lee, S.Y., 2019. Histone deacetylase 6 inhibitor tubastatin A attenuates angiotensin II-induced hypertension by preventing cystathionine γ-lyase protein degradation. Pharmacol. Res. 146, 104281.

Choi, B.-M., Kim, B.-R., 2008. Upregulation of heme oxygenase-1 by brazilin via the phosphatidylinositol 3-kinase/Akt and ERK pathways and its protective effect against oxidative injury. Eur. J. Pharmacol. 580, 12–18.

Correa, F., Mallard, C., Nilsson, M., Sandberg, M., 2011. Activated microglia decrease histone acetylation and Nrf2-inducible anti-oxidant defence in astrocytes: restoring effects of inhibitors of HDACs, p38 MAPK and GSK3β. Neurobiol. Dis. 44, 142–151.

Dong, W., Jia, Y., Liu, X., Zhang, H., Li, T., Huang, W., Chen, X., Wang, F., Sun, W., Wu, H., 2017. Sodium butyrate activates NRF2 to ameliorate diabetic nephropathy possibly via inhibition of HDAC. J. Endocrinol. 232, 71–83.

Gallo, P., Latronico, M.V., Gallo, P., Grimaldi, S., Borgia, F., Todaro, M., Jones, P., Gallinari, P., De Francesco, R., Ciliberto, G., Steinkuhler, C., Esposito, G., Condorelli, G., 2008. Inhibition of class I histone deacetylase with an apicidin derivative prevents cardiac hypertrophy and failure. Cardiovasc. Res. 80, 416–424.

Hannan, J.L., Kutlu, O., Stopak, B.L., Liu, X., Castiglione, F., Hedlund, P., Burnett, A.L., Bivalacqua, T.J., 2014. Valproic acid prevents penile fibrosis and erectile dysfunction in cavernous nerve-injured rats. J. Sex. Med. 11, 1442–1451.

Hausenloy, D.J., Lim, S.Y., Ong, S., Davidson, G.S.M., Yellon, D.M., 2010. Mitochondrial cyclophilin-D as a critical mediator of ischaemic preconditioning. Cardiovasc. Res. 88, 67–74.

Hsu, Y.F., Sheu, J./R., Lin, C.H., Chen, W.C., Hsiao, G., Ou, G., Chiu, P.T., Hsu, M.J., 2011. MAPK phosphatase-1 contributes to trichostatin A inhibition of cyclooxygenase-2 expression in human umbilical vascular endothelial cells exposed to lipopolysaccharide. Biochim. Biophys. Acta 1810, 1160–1169.

Iles, K.E., Dickinson, D.A., Wigley, A.F., Welty, N.E., Blank, V., Forman, H.J., 2005. HNE increases HO-1 through activation of the ERK pathway in pulmonary epithelial cells. Free Rad. Biol. Med. 39, 355–364.

Juhaszova, M., Zorov, D.B., Yaniv, Y., Nuss, H.B., Wang, S., Sollott, S.J., 2009. Role of Glycogen synthase kinase-3β in cardioprotection. Circ. Res. 104, 1240–1252.

Kang, S.H., Seok, Y.M., Song, M.J., Lee, H.A., Kurz, T., Kim, I., 2015. Histone deacetylase inhibition attenuates cardiac hypertrophy and fibrosis through acetylation of mineralocorticoid receptor in spontaneously hypertensive rats. Mol. Pharmacol. 87, 782–791.

Kessler-Icekson, G., Sperling, O., Rotem, C., Wasserman, L., 1984. Cardiomyocytes cultured in serum-free medium. Growth and creatine kinase activity. Exp. Cell Res. 155, 113–120.

Kessler-Icekson, G., Hochhauser, E., Sinai, T., Kremer, A., Dick, J., Tarasenko, N., Nudelman, V., Schlesinger, H., Abraham, S., Nudelman, A., Rephaeli, A., 2012. A histone deacetylase inhibitory prodrug - butyroyloxymethyl diethyl phosphate - protects the heart and cardiomyocytes against ischemia injury. Eur. J. Pharmaceut. Sci. 45, 592–599.

Kliminski, V., Uziel, O., Kessler-Icekson, G., 2017. Popdc1/Bves functions in the preservation of cardiomyocyte viability while affecting Rac1 activity and Bnip3 expression. J. Cell. Biochem. 118, 1505–1517.

Koko, K.R., Chang, S., Hagaman, A.L., Fromer, M.W., Nolan, R.S., Gaughan, J.P., Zhang, P., Carpenter, J.P., Brown, S.A., Matthews, M., Bird, D., 2017. Histone deacetylase inhibitors enhance cytotoxicity towards breast tumors while preserving the wound-healing function of adipose-derived stem cells. Ann. Plast. Surg. 78, 728–735.

Lenčo, J., Lenčová-Popelová, O., Link, M., Jirkovská, A., Tambor, V., Potůčková, E., Stulík, J., Šimůnek, T., Štěrba, M., 2015. Proteomic investigation of embryonic rat heart-derived H9c2 cell line sheds new light on the molecular phenotype of the popular cell model. Exp. Cell Res. 339, 174–186.

Liu, D., Yi, B., Liao, Z., Tang, L., Yin, D., Zeng, S., Yao, J., He, M., 2014. 14-3-3gamma protein attenuates lipopolysaccharide-induced cardiomyocytes injury through the Bcl-2 family/mitochondria pathway. Int. Immunopharm. 21, 509–515.

McKinsey, T.A., Olson, E.N., 2004. Cardiac histone acetylation–therapeutic opportunities abound. Trends Genet. 20, 206–213.

Nural-Guvener, H.F., Zakharova, L., Nimlos, J., Popovic, S., Mastroeni, D., Gaballa, M.A., 2014. HDAC class I inhibitor, Mocetinostat, reverses cardiac fibrosis in heart failure and diminishes CD90+ cardiac myofibroblast activation. Fibrogenesis Tissue Repair 7, 10. https://doi.org/10.1186/1755-1536-7-10.

Pang, M., Kothapally, J., Mao, H., Tolbert, E., Ponnusamy, M., Chin, Y.E., Zhuang, S., 2009. Inhibition of histone deacetylase activity attenuates renal fibroblast activation and interstitial fibrosis in obstructive nephropathy. Am. J. Physiol. Ren. Physiol. 297, F996–F1005.

Park, K.C., Park, J.H., Jeon, J.Y., Kim, S.Y., Kim, J.M., Lim, C.Y., Lee, T.H., Kim, H.K., Lee, H.G., Kim, S.M., Kwon, H.J., Suh, J.S., Kim, S.W., Choi, S.H., 2014. A new histone deacetylase inhibitor improves liver fibrosis in BDL rats through suppression of hepatic stellate cells. Br. J. Pharmacol. 171, 4820–4830.

Rahmani, M., Reese, E., Dai, Yun, Bauer, C., Payne, S.G., Dent, Paul, Spiegel, S., Grant, S., 2005. Coadministration of histone deacetylase inhibitors and perifosine synergistically induces apoptosis in human leukemia cells through Akt and ERK1/2 inactivation and the generation of ceramide and reactive oxygen species. Canc. Res. 65, 2422–2432.

Renaud, L., Harris, L.G., Mani, S.K., Kasiganesan, H., Chou, J.C., Baicu, C.F., Van Laer, A., Akerman, A.W., Stroud, R.E., Jones, J.A., Zile, M.R., Menick, D.R., 2015. HDACs regulate miR-133a expression in pressure overload-induced cardiac fibrosis. Circ. Heart Fail. 8, 1094–1104.

Rephaeli, A., Waks-Yona, S., Nudelman, A., Tarasenko, I., Tarasenko, N., Phillips, D.R., Cutts, S.M., Kessler-Icekson, G., 2007. Anticancer prodrugs of butyric acid and formaldehyde protect against doxorubicin-induced cardiotoxicity. Br. J. Canc. 96, 1667–1674.

Ryter, S.W., Otterbein, L.E., Morse, D., Choi, A.M., 2002. Heme oxygenase/carbon monoxide signaling pathways: regulation and functional significance. Mol. Cell. Biochem. 234–235, 249–263.

Ryter, S.W., Alam, J., Choi, A.M., 2006. Heme oxygenase-1/carbon monoxide: from basic science to therapeutic applications. Physiol. Rev. 86, 583–650.

Salinas, M., Wang, J., Rosa De Sagarra, M., Martín, D., Rojo, A.I., Martin-Perez, J., Ortiz De Montellano, P.R., Cuadrado, A., 2004. Protein kinase Akt/PKB phosphorylates heme oxygenase-1 in vitro and in vivo. FEBS Lett. 578, 90–94.

Seki, M., LaCanna, R.J., Powers, C., Vrakas, C., Liu, F., Berretta, R., Chacko, G., Holten, J., Jadiya, P., Wang, T.J., Arkles, S., Copper, J.M., Houser, S.R., Huang, J., Patel, V., Recchia, F.A., 2016. Class I histone deacetylase inhibition for the treatment of sustained atrial fibrillation. J. Pharmacol. Exp. Therapeut. 358, 441–449.

Shalitin, N., Schlesinger, H., Levy, M.J., Kessler, E., Kessler-Icekson, G., 2003. Expression of procollagen C-proteinase enhancer in cultured rat heart fibroblasts: evidence for co-regulation with type I collagen. J. Cell. Biochem. 90, 397–407.

Sharma, A., Sinha, N.R., Siddiqui, S., Mohan, R.R., 2015. Role of 5'TG3'-interacting factors (TGIFs) in vorinostat (HDAC inhibitor)-mediated corneal fibrosis inhibition. Mol. Vis. 21, 974–984.

Sinha, K., Das, J., Pal, P.B., Sil, P.C., 2013. Oxidative stress: the mitochondria-dependent and mitochondria-independent pathways of apoptosis. Arch. Toxicol. 87, 1157–1180.

Spange, S., Wagner, T., Heinzel, T., Kramer, O.H., 2009. Acetylation of non-histone proteins modulates cellular signalling at multiple levels. Int. J. Biochem. Cell Biol. 41, 185–198.

Tarasenko, N., Cutts, S.M., Phillips, D.R., Inbal, A., Nudelman, A., Kessler-Icekson, G., Rephaeli, A., 2012a. Disparate impact of butyroyloxymethyl diethylphosphate (AN-7), a histone deacetylase inhibitor, and doxorubicin in mice bearing a mammary tumor. PloS One 7, e31393.

Tarasenko, N., Kessler-Icekson, G., Boer, P., Inbal, A., Schlesinger, H., Phillips, D.R., Cutts, S.M., Nudelman, A., Rephaeli, A., 2012b. The histone deacetylase inhibitor butyroyloxymethyl diethylphosphate (AN-7) protects normal cells against toxicity of anticancer agents while augmenting their anticancer activity. Invest. N. Drugs 30, 130–143.

Tarasenko, N., Nudelman, A., Rozic, G., Cutts, S.M., Rephaeli, A., 2017. Effects of histone deacetylase inhibitory prodrugs on epigenetic changes and DNA damage response in tumor and heart of glioblastoma xenograft. Invest. N. Drugs 35, 412–426.

Travers, J.G., Kamal, F.A., Robbins, J., Yutzey, K.E., Blaxall, B.C., 2016. Cardiac fibrosis. Circ. Res. 118, 1021–1040.

Wang, B., Zhu, X., Kim, Y., Li, J., Huang, S., Saleem, S., Li, R.C., Xu, Y., Dore, S., Cao, W.,

2012. Histone deacetylase inhibition activates transcription factor Nrf2 and protects against cerebral ischemic damage. Free Rad. Biol. Med. 52, 928–936.
Wang, G., Hamid, T., Keith, R.J., Zhou, G., Partridge, C.R., Xiang, X., Kingery, J.R., Lewis, R.K., Li, Q., Rokosh, D.G., Ford, R., Spinale, F.G., Riggs, D.W., Srivastava, S., Bhatnagar, A., Bolli, R., Prabhu, S.D., 2010. Cardioprotective and antiapoptotic effects of heme oxygenase-1 in the failing heart. Circulation 121, 1912–1925.
Yao, J., Qian, C.J., Ye, B., Zhang, X., Liang, Y., 2012. ERK inhibition enhances TSA-induced gastric cancer cell apoptosis via NF-kappaB-dependent and Notch-independent mechanism. Life Sci. 91, 186–193.
Zhao, T.C., Cheng, G., Zhang, L.X., Tseng, Y.T., Padbury, J.F., 2007. Inhibition of histone deacetylases triggers pharmacologic preconditioning effects against myocardial ischemic injury. Cardiovasc. Res. 76, 473–481.
Zhu, Q.Y., Wang, Z., Ji, C., Cheng, L., Yang, Y.L., Ren, J., Jin, Y.H., Wang, Q.J., Gu, X.J., Bi, Z.G., Hu, G., Yang, Y., 2011. C6-ceramide synergistically potentiates the anti-tumor effects of histone deacetylase inhibitors via AKT dephosphorylation and alpha-tubulin hyperacetylation both in vitro and in vivo. Cell Death Dis. 2, e117.